An investigation of the sound field above a surface with periodic roughness

Conference or Workshop Item

MADRID
inter.noise 2019
June 16 - 19
NOISE CONTROL FOR A BETTER ENVIRONMENT

An Investigation of the Sound Field Above a Surface with Periodic Roughness

Stronach, Alexander[1]
The Open University
Walton Hall, Milton Keynes, MK7 6AA

Taherzadeh, Shahram[2]
The Open University
Walton Hall, Milton Keynes, MK7 6AA

Attenborough, Keith[3]
The Open University
Walton Hall, Milton Keynes, MK7 6AA

ABSTRACT

When audio-frequency sound is incident near grazing on acoustically-hard surfaces with periodic sub-wavelength roughness air-borne acoustic surface waves are generated which could be used to amplify acoustic signals and, therefore, improve detection ranges of, perimeter security systems. Experimental and numerical studies using the Boundary Element Method (BEM) of the sound field generated over periodically-spaced rectangular strips also show several enhancements as a result of complex interactions between the sound field and the rough surface. Surface waves result in excess attenuation spectra with anomalous maxima greater than the 6.02 dB that would be expected from constructive interference above a smooth acoustically rigid surface. The enhancements are found to depend on the roughness spacing and can be attributed to effects due to the finite width and periodicity of the array, quarter-wavelength resonances in the gaps between elements and Bragg diffraction. Pressure maps of the total sound field over rough surfaces show the details of the sound field at the frequencies of interest. As well as being useful for amplifying frequencies arriving at a sensor array, detailed study of the enhancements provides understanding of the evolution of the sound field over rough surfaces.

Keywords: Noise, Roughness, Metamaterials
I-INCE Classification of Subject Number: 30

[1] alex.stronach@open.ac.uk
[2] shahram.taherzadeh@open.ac.uk
[3] keith.attenborough@open.ac.uk

1. INTRODCUTION

The theoretical formulation of the sound field above a rough surface was undertaken by Tolstoy [1]. He studied the coherent scattering of spherical pulses by applying a small roughness boundary condition developed by Biot. Coherent scatter is more important than incoherent scatter if the size of the roughness elements is much less than the wavelength of the incident sound. Biot replaced the scattering elements with a smooth distribution of dipole and monopole sources under the condition that the centre-to-centre spacing between consecutive roughness elements is small compared to the wavelength of the incident sound. Tolstoy's solution, using a simple effective boundary condition, contains two independent arrivals: a body wave and a surface wave. This surface wave is similar to that predicted by Brekhovskikh [2] over a comb-like impedance surface and was found to decrease exponentially in amplitude with height above the surface and spread cylindrically.

Tolstoy also found that for rigid hemispherical bosses under far-field, near-grazing conditions, the normalised spectrum of the scattered wave is given by,

$$P_s = \frac{\varsigma}{2\pi} k^2 \left[\theta^2 + \frac{2\pi}{kr} \exp\left[-2\varsigma k^2 \left(z + z_0 \right) \right] + 2 \left(\frac{2\pi}{kr} \right)^{1/2} \theta \sin\left(kr - \frac{\pi}{4} \right) \exp\left[-\varsigma k^2 \left(z + z_0 \right) \right] \right]^{1/2} \tag{1.1}$$

where k is the wavenumber, r is the range and $\theta = \tan^{-1}\left[\left(z + z_0 \right) / r \right]$ with z and z_0 being the receiver and source heights respectively. The term ς is the scattering parameter which has units of length and is proportional to the volume per unit area of the elements and is a function of the shape and packing density of the roughness elements. At grazing angles, the scattered wave is the surface wave and is given by,

$$P_B = \varsigma \left(2\pi r \right)^{-1/2} k^{3/2} \tag{1.2}$$

The above case was studied by experimentally by Medwin *et al.* [3] For hemispheres and spherical bosses, the direct wave in the half-space is $P_D = \left(2\pi r \right)^{-1}$ so that,

$$\frac{P_B}{P_D} = \varsigma \left(2\pi r \right)^{1/2} k^{3/2} \tag{1.3}$$

Short range experiments in which spherical pulses were propagated over hemispherical and spherical bosses show that the spectral slope of the resulting boundary waves did obey the $k^{3/2}$ and $r^{1/2}$ dependence expected from equation 2. However, at longer ranges the results deviated from this relationship. The boundary wave amplitude did not continue to grow as predicted in equation 2 but instead tended towards a constant value.

One explanation for this discrepancy is that after a certain range, incoherent scatter dominates. A second explanation suggests that after a certain range, the phase lag between the scattered elements and the direct response results in destructive interference between the two contributions. Similar measurements were carried out over cylinders and assumed to obey the same relationships. However, once again, discrepancies arose in longer-range measurements as a result of multiple diffraction contributions due to the widely-spaced elements. Finally, measurements were carried out over a variety of wedges. The ratio of boundary wave amplitude to direct wave amplitude increases linearly with volume/area and increases with increasing slope of the wedge size. For long range measurements, the ratio asymptotically approaches a constant value which supports the idea that the boundary wave 'self-destructs' due to destructive interference with the direct contributions.

Further analysis into coherent sound scatter from different roughness element shapes was carried out by Tolstoy [4] who determined that in a general case, the boundary wave is a result of energy stored between closely packed roughness elements and exchanged with the compressional energy from the source, resulting in horizontally propagating modes.

The use of poroelastic and rough surfaces for noise control has been well established in both literature and practise. It has been shown by Bashir *et al.* [5] that a surface composed of periodically-spaced rectangular strips can be modelled as a hard-backed slit-pore impedance layer with an effective porosity and flow resistivity determined from the width of the strips and the spacing between them. This is true if the spacing between the elements is less than 50% of the layer depth. This allows for the use of simple and cost-effective arrangements for noise mitigation. However, it has also been found that the same arrays of roughness elements provide sound enhancement at some frequencies. Some of the physical mechanisms that provide such enhancement and attenuation over rib-like structures has been outlined by Bougdah *et al.* [6]. These mechanisms include surface wave generation at lower frequencies, the potential for constructive and destructive interference between scattered contributions, interference within the grooves and also effects due to quarter-wavelength resonances arising within the gaps between elements.

In this paper, the sound field generated over a surface composed of periodically-spaced rectangular strips is investigated both experimentally and numerically, as is the effect of varying the spacing between the strips on the enhancement features observed in excess attenuation spectra.

2. SLIT-PORE IMPEDANCE MODEL

A comb-like surface made from parallel rectangular strips can be considered to act acoustically as a hard-backed locally reacting rigid porous layer composed of slit-like pores [5]. The slit-pore impedance model is applicable where viscous and thermal boundary layers exist due to sound propagation between the slits. The ground may be characterised by a complex density $\rho(\omega)$, and a complex compressibility $C(\omega)$,which account for the viscous and thermal effects respectively.

$$\rho(\omega) = \frac{\rho_0}{H(\lambda)} \tag{2.1}$$

$$C(\omega) = \frac{1}{\gamma\rho_0}\left[\gamma - (\gamma-1)H\left(\lambda\sqrt{N_{PR}}\right)\right] \tag{2.2}$$

$$H(\lambda) = 1 - \frac{\tanh\left(\lambda\sqrt{-i}\right)}{\lambda\sqrt{-i}}, \lambda = \sqrt{\frac{3\omega\rho_0 T}{\Omega R_s}} \tag{2.3}$$

The function $H(\lambda)$ is the complex density function, $\left(\gamma\rho_0\right)^{-1}$ is the adiabatic compressibility of air, γ is the ratio of specific heats, N_{PR} is the Prandtl number, Ω is the porosity and R_s is the flow resistivity. The dimensionless parameter λ can be related to the flow resistivity of the bulk material using the Kozeny-Carman formula,

$$R_s = \frac{2\mu T s_0}{\Omega r_h^2} \tag{2.4}$$

where T is the tortuosity (T = 1 for vertical slits), μ is the viscosity, s_0 is the pore shape factor (s_0 =1.5 for slit-like pores) and r_h is the hydraulic radius which can be taken to be half the value of the edge-to-edge spacing, between roughness elements.

The bulk propagation constant, $k(\omega)$and the relative characteristic impedance, $Z_c(\omega)$ can be written as,

$$k(\omega) = \omega\sqrt{T\rho(\omega)C(\omega)} \tag{2.5}$$

$$Z_c(\omega) = \frac{1}{\rho_0 c_0}\sqrt{\left(\frac{T}{\Omega^2}\right)\frac{\rho(\omega)}{C(\omega)}} \tag{2.6}$$

3. METHODS

3.1 Modelling

The results in this paper are obtained using simulations of the sound field over the surfaces of interest via a 2D Boundary Element Method (BEM) program developed by Taherzadeh *et al.* [7]. The boundary element method solves partial differential equations formulated as boundary integrals. Through the implementation of boundary conditions, the sound field can be found at any point within a specified domain of interest. The program developed by Taherzadeh has the benefit of not requiring discretisation of the ground surface since it is possible to simply define the impedance parameters of that surface instead. As a result, the computational time is significantly reduced.

The above program is useful for the study of excess attenuation spectra in the frequency domain. It is possible to identify enhancement features in excess attenuation spectra since the maximum possible enhancement as a result of constructive interference due to reflection from an acoustically rigid surface is 6.02 dB. Therefore, any excess attenuation peak above this value is of interest.

3.2 Simulation Setup

The elements have a fixed height of 0.02 m. The element thickness is varied between 0.01 m, 0.03 m, 0.06 m and 0.10 m. This has been done for strip spacings of 0.005 m, 0.02 m, 0.03 m and 0.04 m.

The source and receiver are separated by 1.00 m and their heights are kept constant at 0.03 m so that they sit 0.01 m above the strip surface. The source sits just above the first strip and the receiver is just outside the array.

4. RESULTS & DISCUSSION

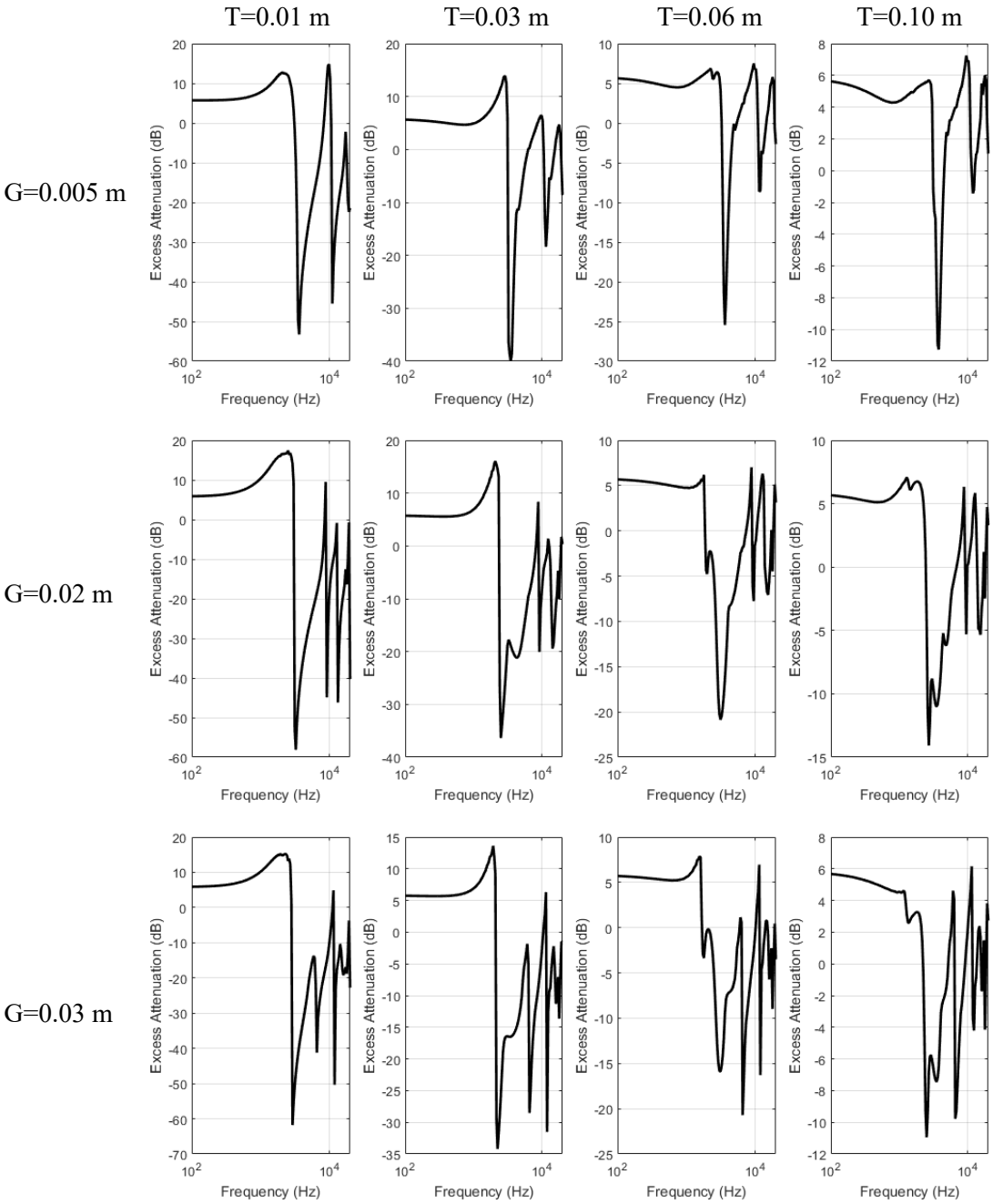

G=0.04 m

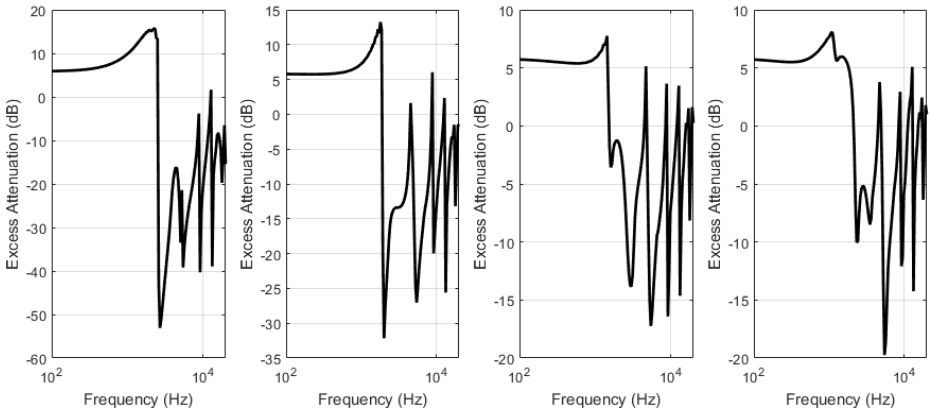

Figure 1. *Excess attenuation spectra as a function of frequency for strips with a varying thickness, T for a given spacing, G.*

For the smallest spacing, the surface appears to act as a slit-pore impedance layer due to the width of the gaps being less than 50% of the strip height (layer depth). Thus the peak above 6.02 dB can be attributed to the generation of an air-borne acoustic surface wave. This is characterizable by the broadness of the peak and is caused by a high 'springlike' reactance associated with the effective impedance of the surface. As the gap (and effective porosity associated with the surface) is increased, the reactance reduces.

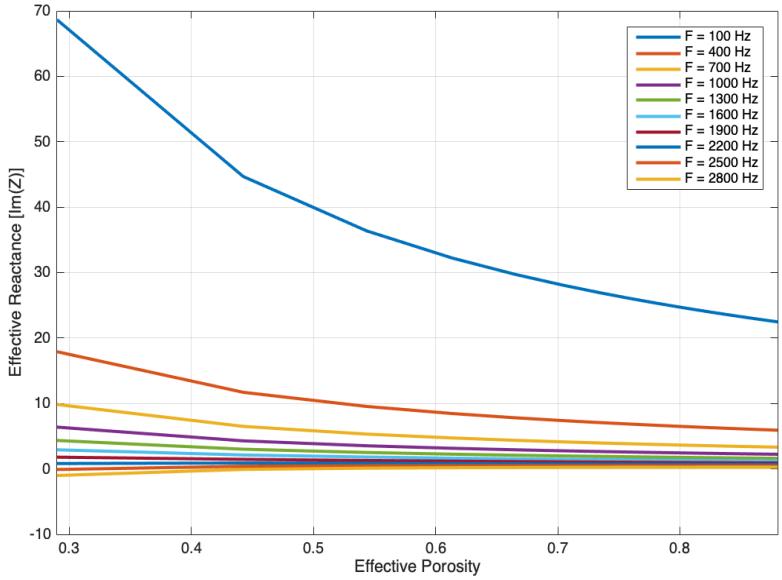

Figure 2. *Effective reactance at various frequencies of a strip surface as a function of the effective porosity. The strips have a height of 0.02 m (layer depth) and a thickness of 0.01 m.*

As the gap is increased, the surface begins to behave more as a rough surface and the peak in the excess attenuation spectrum becomes sharper. This is because the roughness elements begin to act as individual scatterers. A second peak becomes more dominant and thus the enhancement feature can no longer be attributed to a surface wave.

The enhancement achieved by a rough surface is dependent on the number of scattering edges per wavelength. For smaller gaps, the number of edges per wavelength is higher resulting in more diffracted contributions at the receiver constructively interfering and providing sound enhancement. Once the number of scattering edges is reduced and the spacing is increased, quarter-wavelength resonances arise within the gaps. This is similar to the effect observed in organ pipes closed at one end and the associated end correction can be calculated using,

$$f_{qwr} = \frac{c}{4\left(h + E\right)} \tag{4.1}$$

where h is the strip height and E is an end correction.

Thickness (m)	0.005	0.02	0.03	0.04
Gap (m)	End Correction	End Correction	End Correction	End Correction
0.01	0.0205	0.0089	0.0115	0.0118
0.03	0.0171	0.0163	0.0205	0.0180
0.06	0.0182	0.0252	0.0268	0.0361
0.10	0.0345	0.0441	0.0474	0.0529

Table 1. *The end corrections associated with each spacing and thickness.*

The end correction for an unflanged circular pipe is approximately $0.3G$ [8]. Table 1 shows the end corrections are larger for smaller gaps between strips. It is thought that this is due to interactions between the resonances resulting in regions of higher pressure. As the gap is increased, these resonances cease to interact and the end correction decreases and becomes closer to the accepted value of 0.3 times the gap. Simulations carried out for the total sound field over the strips at the frequency of the excess attenuation maximum show this. For a fixed source-receiver separation of 1.0 m, the number of strips was varied between 40 strips with a separation of 0.0178 m and 23 strips with a separation of 0.0534 m.

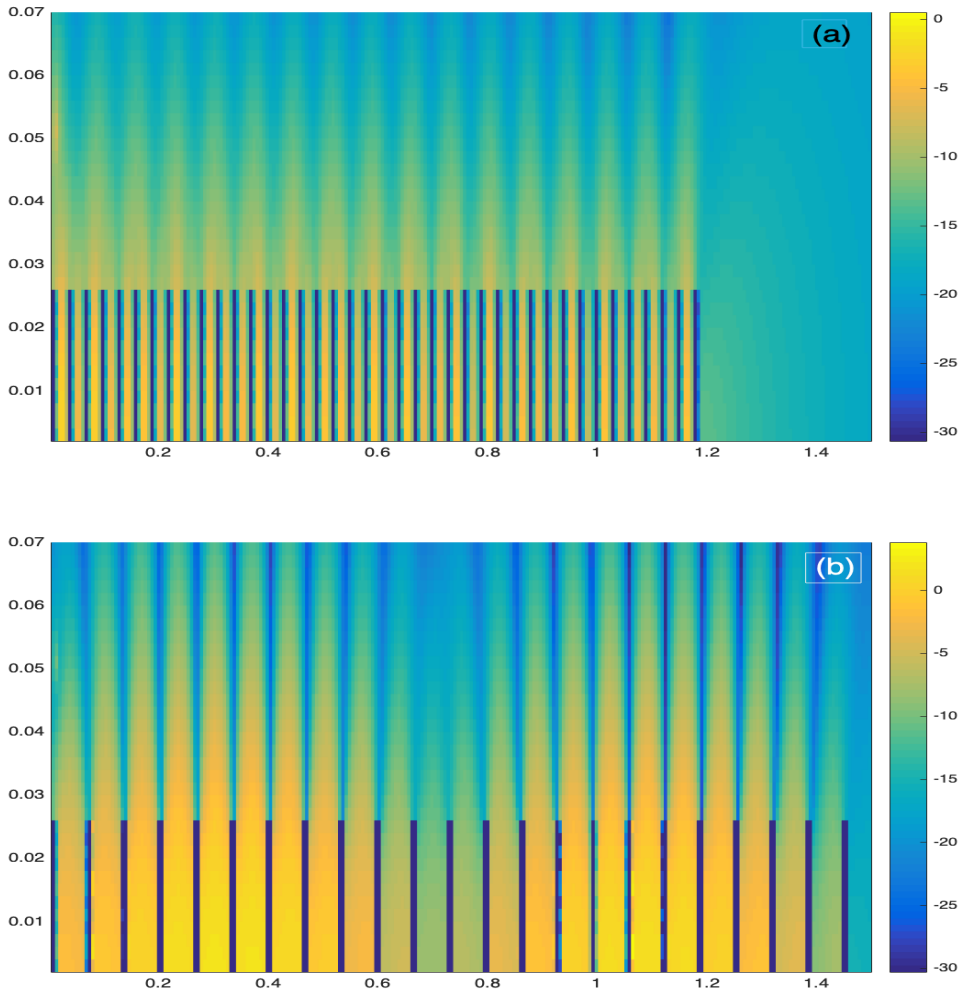

Figure 3. *(a) Total sound field over 40 periodically-spaced rectangular strips at frequency of enhancement feature (1951 Hz) (b) Total sound field over 23 periodically-spaced rectangular strips at frequency of enhancement feature (1857 Hz).*

Figure 3 shows that as the gap is decreased, the high pressure regions begin to interact. This is identifiable as the high pressure region every 3 strips. For the larger gap, a high pressure region can be seen above every strip since these resonances can no longer interact.

As the gap is increased so that there are less than 3 edges per wavelength, the enhancement features can be attributed to Bragg-like diffraction effects. Bragg diffraction occurs when two diffracted wave scatter coherently from points on a crystal lattice, in this case the roughness element edges. These waves interfere both constructively and destructively depending on the path length difference between them. The Bragg frequencies, f_{br} at which interference occurs is derived from Bragg's law and is given by,

$$f_{br} = \frac{c_0 n}{2b\sin\alpha} \quad , \quad n = 1,2,3... \tag{4.2}$$

To investigate the Bragg-diffraction effect, a series of simulations was carried out for large strip separations with an increased source-receiver geometry. The source-receiver separation was set at 2.00 m and the source and receiver heights were set at 0.03 m. The thickness and height of the strips were 0.04 m and 0.02 m respectively. The gaps were set at 0.125 m, 0.25 m and 0.5 m corresponding to 13, 7 and 5 strips, respectively. The geometry was chosen such that there was one element per wavelength which is in agreement with Bragg theory.

Gap (m)	**First Bragg Frequency (Hz) (n=1)**	**First Excess Attenuation Peak frequency (Hz)**
0.125	1039	950
0.250	591	523
0.500	318	281

Table 2. *Frequency of first excess attenuation peak for a strip gaps of 0.125 m, 0.250 m, and 0.500 m and the corresponding Bragg diffraction frequencies calculated from equation 6.25.*

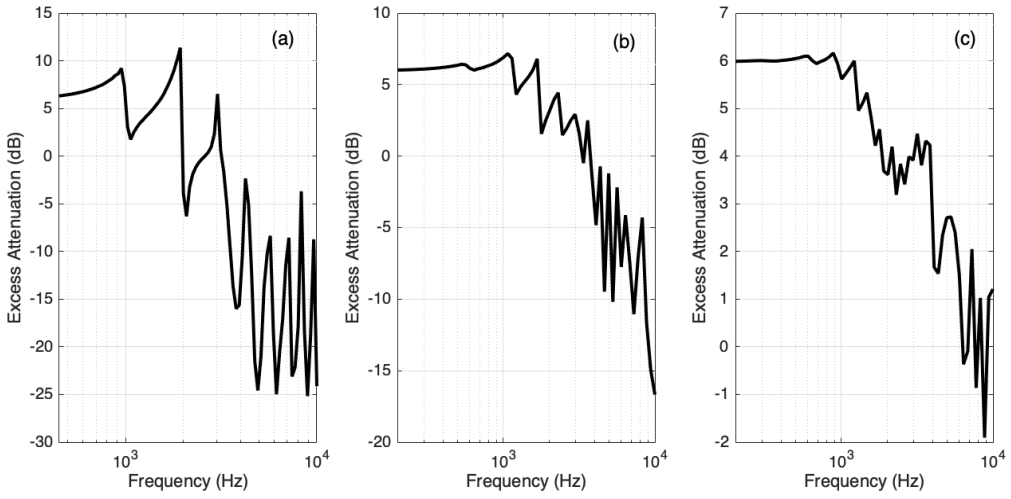

Figure 3. *(a) Excess attenuation spectrum for 13 strips with an edge-to-edge spacing of 0.0125 m. (b) Excess attenuation spectrum for 7 strips with an edge-to-edge spacing of 0.250 m (c) Excess attenuation spectrum for 4 strips with an edge-to-edge spacing of 0.500 m*

There is good agreement between the frequencies of the first peaks in the excess attenuation spectra and the Bragg frequencies calculated from the geometry associated with the spectra.

One assumption in Bragg theory is that the periodicity remains constant between scattering elements. In order to investigate the effect on the sound field of aperiodicity, the spacing between elements was randomised. The results are displayed in figure 4 and it is clear to see that the peaks due to Bragg diffraction have diminished. The peaks in the spectra are a result of constructive interference between scattered waves from the tops of the strips and it is also clear that the amplification potential of such an array is inferior to that of a periodic array.

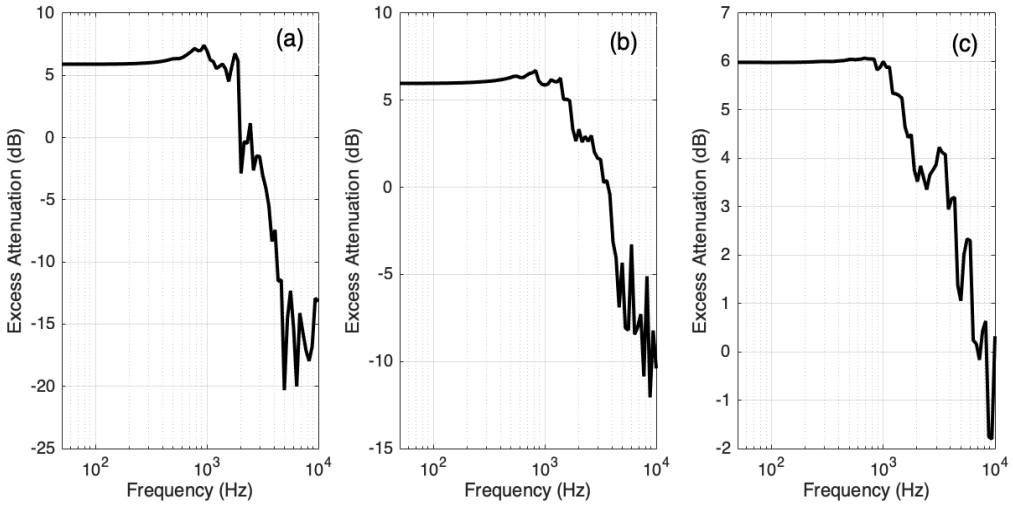

Figure 4. *(a) Excess attenuation spectrum for 13 strips with randomised spacing(b) Excess attenuation spectrum for 7 strips with randomised spacing (c) Excess attenuation spectrum for 4 strips with randomised spacing.*

5. CONCLUSIONS

The sound field generated over a surface composed of periodically-spaced strips has been investigated via numerical simulation. Plots of excess attenuation show distinct enhancement peaks above the 6.02 dB associated with constructive interference due to total reflection off an acoustically rigid surface. The mechanisms by which these enhancements are generated vary with the spacing between roughness elements.

For smaller spacings, the surface behaves like a slit-pore impedance layer with a high imaginary impedance resulting in the generation of an air-borne acoustic surface wave. This is also due to a high number of scattering edges per wavelength which give rise to diffracted contributions that constructively interfere at the receiver. As the gap increases and the number of scattering edges per wavelength decreases, quarter-wavelength resonances arise within the gaps. These resonances interact when the gap is smaller and produce high pressure regions above the strip array resulting in enhancement.

As the gap is increased further and the number of edges per wavelength reduces to less than 3, the dominant enhancement mechanism becomes Bragg diffraction. This phenomena only arises when the roughness elements are periodic. This is useful since it shows sound enhancement is achievable with very few roughness elements. However, the more scattering edges per wavelength, the stronger the enhancement.

REFERENCES

[1] I. Tolstoy (1979), 'The scattering of spherical pulses by slightly rough surfaces,' *J. Acoust. Soc. Am*, **66** (4), 1135 – 1144

[2] L. M. Brekhovskikh (1960), 'Surface waves in acoustics,' *Sov. Phys. Acoust,* **5**, 3 – 12

[3] H. Medwin, G. L. D'Spain, E. Childs, S. J. Hollis (1984), 'Low-frequency grazing propagation over periodic steep-sloped rigid roughness elements,' *J. Acoust. Soc. Am,* **76** (6), 1774 – 1790

[4] I. Tolstoy (1981), 'Coherent sound scatter from a rough interface between arbitrary fluids with particular reference to roughness element shapes and corrugated surfaces,' *J. Acoust. Soc. Am,* **72** (3), 960 – 972

[5] I. Bashir, S. Taherzadeh, K. Attenborough (2013), 'Surface waves over periodically-spaced strips,' *J. Acoust. Soc. Am,* **134** (6), 4691 – 4697

[6] H. Bougdah, I. Ekici, J. Kang (2006), 'A laboratory investigation of noise reduction by riblike structures on the ground', *J. Acoust. Soc. Am,* **120** (6), 3714 – 3722

[7] S. Taherzadeh, K. M. Li, K. Attenborough (2001), 'A Hybrid BIE/FFP scheme for predicting barrier efficiency outdoors,' *J. Acoust. Soc. Am*, **110** (2), 918

[8] H. Levine, J. Schwinger (1948), 'On the radiation of sound from an unflanged circular pipe,' *Physical Review,* **73** (4), 383 – 406